A High-Pressure Droplet Model for Spray Simulations

Changlin Yan

Suresh K. Aggarwal[1]
e-mail: ska@uic.edu

Department of Mechanical Engineering,
University of Illinois at Chicago,
842 West Taylor Street, MC 251,
Chicago, IL 60607-7022

Droplet vaporization models that are currently employed in simulating sprays are based on a quasisteady, low-pressure formulation. These models do not adequately represent many high-pressure effects, such as nonideal gas behavior, solubility of gases into liquid, pressure dependence of gas- and liquid-phase thermophysical properties, and transient liquid transport in the droplet interior. In the present study, a high-pressure quasisteady droplet vaporization model is developed for use in comprehensive spray simulations for which more rigorous vaporization models, such as those based on unsteady formulations, are beyond the present computational capabilities. Except for the gas-phase quasisteady assumption that is retained in the model, the model incorporates all high-pressure effects. The applicability of the model for predicting droplet vaporization in diesel and gas turbine combustion environments is evaluated by comparing its predictions with the available experimental data and with those from a more comprehensive transient model. Results indicate a fairly good agreement between the quasisteady (QS) and transient (TS) models for a wide range of pressures at low ambient temperatures, and for pressure up to the fuel critical pressure at high ambient temperatures. The QS model generally underpredicts the vaporization rate during the earlier part of droplet lifetime and overpredicts during the later part of lifetime compared to those using the TS model, and the difference becomes increasingly more significant at higher ambient pressure and temperature. The differences can be attributed to the quasisteady gas-phase average temperature and composition assumption for the QS model that reduces and increases the gas-phase heat and mass fluxes at the droplet surface during the earlier and later part of lifetime, respectively. The applicability of the QS model is quantified in terms of the maximum pressure as a function of ambient temperature. [DOI: 10.1115/1.1915390]

Introduction

The gasification behavior of a liquid fuel droplet has been a subject of extensive research. This research has been motivated by two major considerations. First, the droplet gasification model provides a fundamental input for the simulation of reacting two-phase flows that typically occur in gas turbine, liquid rocket, and diesel engine combustors. Second, the droplet gasification phenomenon is scientifically challenging as it involves the coupled processes of fluid flow, heat and mass transport, phase change, and interphase coupling. For a combusting droplet, it also involves radiation and chemical reactions.

The basic droplet gasification model was formulated in the 1950s by Godsave [1] and Spalding [2] for an isolated pure fuel droplet in a stagnant environment. This model was termed the d^2-law model as it predicted that the square of the droplet diameter decreases linearly with time. Since then this model has been studied extensively both experimentally and theoretically. Reviews of these studies have been provided by Williams [3], Law [4], Sirignano [5], and Peng and Aggarwal [6]. The key assumptions in the basic model are that the gas-phase processes are quasisteady, the droplet and gas flow are in dynamic equilibrium (zero slip velocity), the droplet surface temperature is constant (droplet heating time is negligible compared to its lifetime), and the thermophysical properties of the gas film surrounding the droplet are invariant. The effects of relaxing these restrictions have been investigated by Law [4], Sirignano [7], Aggarwal et al. [8], and Abramzon and Sirignano [9]. In particular, they have considered the effect of transient liquid-phase heating on the droplet vaporization rate, and proposed four different models with varying degree of complexity to include this effect in the d^2-law model. The four models have been termed, respectively, as the infinite-conductivity or rapid-mixing model, the conduction-limit model, the effective conductivity model, and the vortex model. In addition, the effects of relative gas velocity or forced convection [6,10], multicomponent fuel [4,7,11,12], and variable transport properties [9,12] have been included in the modified d^2-law model.

Except for some variations, the state-of-the-art droplet gasification model that is currently employed in multidimensional spray computations in diesel and gas turbine combustors has the following general features:

1. The assumptions of gas-phase processes being quasi-steady and spherically-symmetric are retained. The effect of transient liquid heating is included by using an infinite conductivity model, whereby the liquid temperature is considered temporally varying but spatially uniform.
2. The effect of relative gas velocity is included by using a semiempirical correlation representing the effects of droplet Reynolds number and Prandtl (or Schmidt) number on the interphase heat and mass transport.
3. The phase equilibrium at the droplet surface is represented by the Clausius-Clapeyron or an equivalent expression.
4. The effects of variable thermophysical properties are incorporated in an ad hoc manner. For example, the effect of temperature on the gas-phase properties, such as specific heat, thermal conductivity, viscosity, and mass diffusivity are included. However, the effect of composition is generally neglected, and the variation of liquid transport properties is not considered.
5. A pure or single-component fuel is considered, although most practical fuels are multicomponent in nature.
6. Many important high-pressure effects are not considered. These include the gas-phase nonidealities, liquid-phase solubility of gases, and variation of gas- and liquid-phase properties with pressure.

[1]To whom correspondence should be addressed.

Contributed by the Combustion and Fuels Division of ASME for publication in the JOURNAL OF ENGINEERING FOR GAS TURBINES AND POWER. Manuscript received August 4, 2003; final manuscript received May 5, 2004. Assoc. Editor: P. C. Malte.

Motivation and Objective

Clearly, a spray code based on the droplet gasification model described above would be inadequate for simulating two-phase flows in high pressure combustors, where the gas temperature and pressure typically exceed the critical temperature and pressure of the fuel. Under such conditions, aspects dealing with the high-pressure and transcritical phenomena become extremely important. In particular, the gas-phase nonidealities and the liquid-phase solubility of gases become essential considerations as pressure approaches the fuel critical value. As a consequence, interphase processes at the droplet surface and liquid-phase processes inside the droplet become significantly more complex. The phase equilibrium at the droplet surface can no longer be represented by Clausius–Clapeyron-type equation. The solubility of gases into liquid implies that a single component fuel behaves like a multicomponent fuel. In addition, the liquid- and gas-phase thermophysical properties become pressure dependent. Since the liquid boiling temperature increases with pressure, the droplet heat-up time becomes a significant part of droplet lifetime, and an infinite-conductivity model may be inadequate to represent the liquid-phase transport inside the droplet. As the droplet surface reaches the critical state, the latent heat of vaporization reduces to zero, and the gas and liquid densities become equal at the droplet surface. Then, transient effects in the gas phase become as important as those in the liquid phase, since the characteristic times for transport processes in the two phases become comparable. These high-pressure effects are not adequately represented in the low-pressure droplet models used in spray codes that are deployed for multidimensional simulations of two-phase flows in diesel engines and gas-turbine combustors.

Motivated by these considerations, the present study aims to develop a high-pressure droplet gasification model, which can replace the low-pressure droplet models that are currently used in high-pressure spray simulations. The new model incorporates the high-pressure effects described above, which are generally not considered in the low-pressure QS models. These include the gas-phase nonidealities, liquid-phase solubility of gases at the droplet surface, pressure dependency of the gas- and liquid-phase thermophysical properties, high-pressure gas- and liquid-phase equilibrium at the droplet surface, and transient transport in the droplet interior. The applicability of the quasisteady model is examined by comparing its predictions with those using a transient droplet model, and with experimental data. Using this comparison, the validity of the quasisteady assumption is quantified for a wide range of ambient pressures and temperatures.

It is important to note that modeling capabilities are currently available to incorporate high-pressure effects described above in a comprehensive, transient droplet gasification model. Issues pertaining to the inclusion of these effects and the various forms of the high-pressure transient models have been studied by several investigators [13–23,26]. However, such transient models, although they are extremely useful to examine the subcritical/supercritical vaporization behavior of a single droplet, cannot be incorporated in practical spray codes, at least in the foreseeable future. Zhu et al. [36] employed a detailed quasisteady model to quantify the gas-phase unsteadiness as a function of ambient pressure and temperature. However, this model is still too complex to be useful for simulating sprays in practical systems. Thus there is a clear need to develop a high-pressure droplet model for the simulation of high-pressure, two-phase flows that are encountered in various propulsion applications. The model should provide a realistic representation of the important high-pressure effects, and still be sufficiently simplified so that it can easily be incorporated into comprehensive spray codes. This provided another motivation for the present study.

In the following, we first present the quasisteady high-pressure droplet model, and its validation using results from experiments and a comprehensive transient droplet model. This is followed by detailed results dealing with the range of applicability of the QS model, the sensitivity of vaporization rate to thermotransport properties, the effect of pressure on these properties, and the quantification of the quasisteady assumption in terms of ambient pressure and temperature. Finally, the conclusions are presented.

The Theoretical Model

Quasi-Steady Gas Phase Model. An isolated fuel droplet evaporating in a high-temperature, high-pressure environment is analyzed. The droplet size, ambient temperature and pressure are considered in a range that corresponds to a wide range of power requirements for diesel and gas turbine combustion. The gas-phase processes are assumed to be quasi-steady, which implies that the characteristic gas-phase time is much shorter compared to the liquid-phase transient time as well as the time associated with the surface regression rate. Other assumptions include spherical symmetry, phase-equilibrium at the droplet surface, and negligible secondary diffusion and radiation. With these assumptions, the energy and fuel-vapor species conservation equations can be simplified to a steady, one-dimensional form, and their solution respectively yields the droplet gasification rate as:

$$\frac{\dot{m}}{4\pi\rho_g D_g Le_g}[1/r_s - 1/r_\infty] = \ln\left[1 + \frac{C_{pg}(T_\infty - T_s)}{H}\right] \tag{1}$$

$$\frac{\dot{m}}{4\pi\rho_g D_g}[1/r_s - 1/r_\infty] = \ln\left[\frac{1 - Y_{f\infty}}{1 - Y_{fs}}\right] \tag{2}$$

Details can be found in Refs. [24,25]. Here r_s and r_∞ represent, respectively, the radial locations at droplet surface and ambient (assumed to be at infinity), Le_g the gas-phase Lewis number, Y_f the fuel vapor mass fraction, and H the energy supplied to the droplet per unit mass of fuel vaporized used for droplet heating and vaporization. Equation (2) can also be written as

$$\frac{\dot{m}}{4\pi\rho_g D_g}[1/r_s - 1/r_\infty] = \ln(1 + B) \tag{3}$$

where B is the transfer number [7] given by

$$B = \frac{Y_{fs} - Y_{f\infty}}{1 - Y_{fs}} \tag{4}$$

Equating Eqs. (1) and (3) yields an expression for H

$$H = \frac{C_{p_g}(T_\infty - T_s)}{(1 + B)^{1/Le_g} - 1} \tag{5}$$

The droplet size history is computed by using the equation

$$\frac{dr_s^2}{dt} = -\frac{\dot{m}}{2\pi r_s \rho_l} \tag{6}$$

Liquid Phase: Diffusion-Limit Model. For this model, which has been extensively discussed in previous studies [4,8,24], the heat and mass transport in the droplet interior are assumed to be governed by the transient heat and mass diffusion equations. Since, these equations involve a moving boundary problem, a transformation is used to cast the moving boundary (droplet surface) into a fixed one. The transformed equations are:

$$\frac{\partial \bar{T}_l}{\partial \bar{t}} = \frac{1}{\bar{r}^2}\frac{\partial}{\partial \bar{r}}\left(\bar{r}^2 \frac{\partial \bar{T}_l}{\partial \bar{r}}\right) - \bar{r}\bar{m}\frac{\rho_g D_g}{\rho_l \alpha_l}\frac{\partial \bar{T}_l}{\partial \bar{r}} \tag{7}$$

with the initial and boundary conditions as

$$\bar{T}_l = 0 \quad \text{at} \quad \bar{t} = 0$$

$$\frac{d\bar{T}_l}{d\bar{r}} = 0 \quad \text{at} \quad \bar{r} = 0$$

$$\frac{\partial \bar{T}_l}{\partial \bar{r}} = \bar{m}\frac{\rho_g D_g}{k_l(T_b - T_0)}(H - L) \quad \text{at} \quad \bar{r} = 1 \tag{8}$$

where, $\bar{T}_l(\bar{r},\bar{t})$, $\bar{r}$, and $\bar{t}$ are the normalized liquid temperature, radial location, and temporal variable respectively. These are given by

$$\bar{T}_l = \frac{(T_l - T_o)}{(T_b - T_o)}$$

$$\bar{r} = r/r_s$$

$$\bar{t} = \alpha_l \int_0^t \frac{dt}{r_s^2}$$

$$\bar{m} = \frac{\dot{m}}{4\pi\rho_g D_g r_s} \tag{9}$$

where T_o is the initial droplet temperature, T_b is a reference boiling temperature, r_s the instantaneous droplet radius, α_l the liquid thermal diffusivity, and $\bar{m}$ is the normalized vaporization rate. A Crank–Nicolson implicit scheme with a variable grid is employed to solve these equations.

Vapor–Liquid Equilibrium at Droplet Surface. For low-pressure models, the phase equilibrium at the droplet surface is represented by the Clausius–Clapeyron or an equivalent expression, relating fuel vapor mass fraction and temperature at the droplet surface. This representation, however, assumes ideal gas behavior and neglects solubility of gases into liquid. In order to include the nonideal gas behavior and gas solubility, which become important at high pressures, various approaches have been suggested [23,26]. Our previous investigation [26] has established that the Peng–Robinson (P–R) equation of state (EOS) provides an accurate representation of the nonideal gas behavior and the vapor-liquid equilibrium at droplet surface. It can be written as

$$P = \frac{RT}{V - b} - \frac{a}{V^2 + 2bV - b^2} \tag{10}$$

where a and b are functions of species properties and mole fractions.

When the droplet surface is in mechanical and thermodynamic equilibrium, the temperature, pressure, and fugacity of each species in the gas phase is equal to the corresponding property of the same species in the liquid phase. The equality of fugacity of species i is expressed as

$$\phi_i^v y_i = \phi_i^l x_i \tag{11}$$

where the superscripts v and l refer to the vapor and liquid phase, respectively. ϕ_i is the fugacity coefficient of ith species, and is a function of pressure, temperature, and composition. It is given in terms of the volumetric properties of the mixture by the following thermodynamic relation:

$$RT\ln(\phi_i) = \int_v^\infty \left[\left(\frac{\partial P}{\partial n_i}\right)_{T,V,n_j} - \frac{RT}{V}\right]dV - RT\ln Z \tag{12}$$

where Z is the compressibility factor, and n_j is the mole number of jth species. By substituting the equation of state into Eq. (12), the fugacity of the ith species in the liquid and gas phase mixture is given by [27]:

$$\ln\phi_i = \frac{bi}{b}(Z - 1) - \ln(Z - B^*) + \frac{A^*}{2B^*\sqrt{2}}\left(\frac{b_i}{b} - \delta_i\right)\ln\frac{Z + B^*(1 + \sqrt{2})}{Z + B^*(1 - \sqrt{2})} \tag{13}$$

where

$$A^* = \frac{aP}{R^2T^2}$$

and

$$B^* = \frac{bP}{RT}$$

$$\frac{b_i}{b} = \frac{T_{ci}/P_{ci}}{\sum_j y_j T_{cj}/P_{cj}} \quad \text{and} \quad \delta_i = \frac{2\sqrt{a_i}}{a}\sum x_j\sqrt{a_j}(1 - k_{ij}) \tag{14}$$

The binary interaction coefficient k_{ij} in the above equation is taken from Knapp et al. [28]. It is 0.1441 for P–R EOS for n-heptane–nitrogen system. Equations (10)–(14) provide the basic relations for vapor–liquid equilibrium calculation.

For a multicomponent mixture, the latent heat of vaporization of each species is defined as the difference between the partial molar enthalpy of that species in the vapor and liquid phases. The following thermodynamic relation then gives the partial molar enthalpy of the kth species:

$$\bar{H}_i - \bar{H}_i^0 = -RT^2\frac{\partial}{\partial T}(\ln\phi_i) \tag{15}$$

where the superscript 0 denotes the quantity in an ideal state. Equation (15) is solved iteratively along with Eqs. (10)–(14).

Thermophysical and Transport Properties. The gas- and liquid-phase thermodynamic and transport properties are considered functions of temperature, pressure and composition. The densities of both gas- and liquid-phase are calculated directly from the P–R EOS. The heat capacity of both phases is calculated by a fourth-order polynomial of temperature, and is then extended to mixtures using the mixing rule of Filippov [29]. The thermal conductivity of pure liquid component is estimated by the Baroncini et al. method [30] followed by the Baroncini et al. correction [27] for the effect of pressure, and is then extended to mixtures using the mixing rule of Filippov [29]. The thermal conductivity of pure gas component is calculated by the method of Chung [31,32], while the method of Mason and Saxena [27] is used for gas mixtures, and the Stiel and Thodos modification [27] is used to consider the effect of pressure. The method of Wilke and Lee [27] is used to estimate the gas binary-diffusion coefficient between n-heptane and nitrogen, and the Takahashi correction [33] is employed to predict its value at high pressure.

All the gas-phase mixture properties are computed at the weighted-averaged temperature and species mass fractions, obtained from the temperature and composition at the droplet surface and those in the gas phase at infinity, as

$$\Phi_{\text{avg}} = \Phi_s + \beta(\Phi_\infty - \Phi_s) \tag{16}$$

where Φ is a generic quantity representing either temperature or mass fraction, and the averaging factor β is selected to be as 1/3. It is important to note that the gas-film thickness changes with time during droplet evaporation, and also varies with ambient properties. Consequently, the averaging factor β should be adjusted accordingly. This aspect is examined using results of the transient droplet model.

The Solution Procedure. The theoretical model described above is applicable to a single isolated fuel droplet. A general procedure involves calculating phase equilibrium at droplet surface by using T_s at the old time step. Then, the average gas temperature and species mass fractions are obtained from Eq. (16), and the thermotransport properties of the gaseous mixture are calculated by using the equations described above. Similarly, the liquid fuel properties, such as specific heat, thermal conductivity, and density, are computed. Note that liquid temperature and species mass fractions used for calculating these properties are the average values obtained using values at the droplet surface and

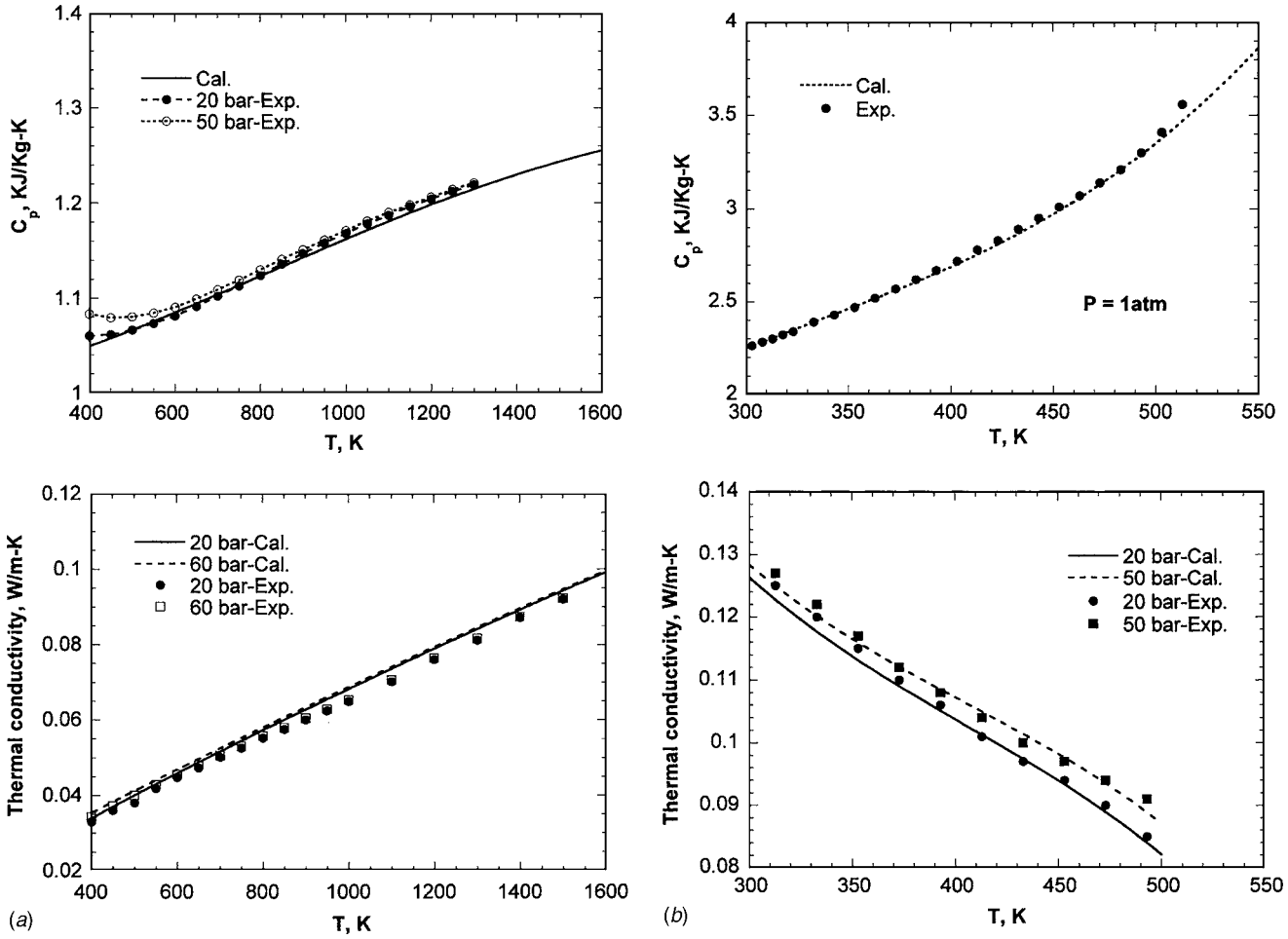

Fig. 1 Comparison of predicted thermophysical and transport properties with measured data; (*a*) gas (nitrogen) properties and (*b*) liquid (*n*-heptane) properties

center. The new T_s is then computed using the diffusion-limit model. Finally, the droplet radius is calculated from Eq. (6).

Results and Discussions

The simulations consider an *n*-heptane droplet evaporating in a nitrogen environment. The environment temperature and pressure are treated as parameters. Results are first presented to validate the methodology used to calculate the thermophysical and transport properties, and the liquid–vapor phase equilibrium. This is followed by the validation of the quasisteady (QS) model by comparing its predictions with the available experimental data and with a detailed transient (TS) model. Detailed results of the QS model and comparisons between the predictions of the QS and TS models are then presented, and the range of applicability of the QS model is quantified.

Model Validation. The gas and liquid-phase thermophysical properties were calculated as functions of temperature and pressure, and compared with the available experimental data [34]. The properties include the density, thermal conductivity, mass diffusivity and specific heat of both the gas and liquid species. Figure 1 shows a comparison of the predicted and measured specific heat and thermal conductivity of nitrogen as well as the specific heat and thermal conductivity of liquid *n*-heptane. The predicted values are in good agreement with the experimental data.

The predicted phase equilibrium using the P–R EOS for a *n*-heptane-nitrogen system as a function of pressure and temperature were compared with the available experimental data [28]. The phase equilibrium in terms of the variation of nitrogen mole fraction with pressure for two different temperatures is presented in Fig. 2. An excellent agreement is indicated between the predicted and experimental results. This also indicates that the densities of both the gas- and liquid-phase can be predicted accurately using P–R EOS. Additional validation of the P–R EOS is provided in Ref. [26].

In Fig. 3, we compare the predictions of quasisteady (QS) and

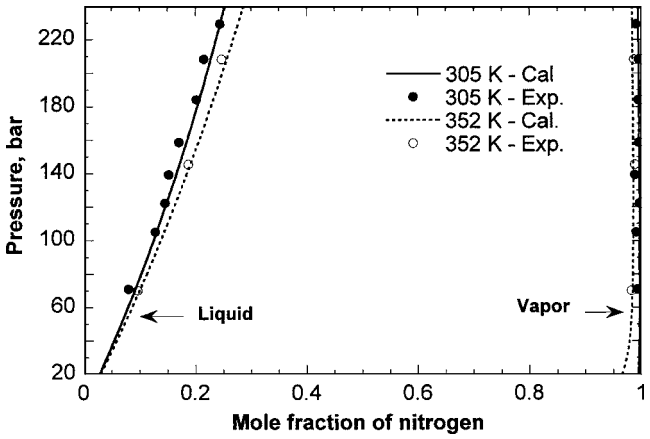

Fig. 2 Comparison of predicted mole fraction of nitrogen with measured data at two different temperatures for an *n*-heptane-nitrogen binary system

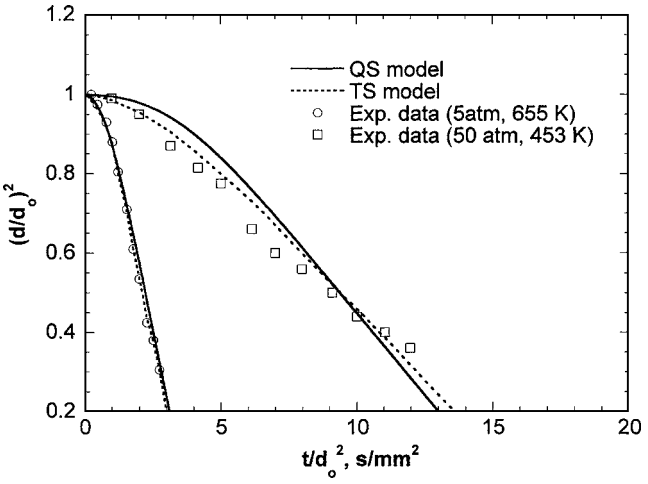

Fig. 3 Temporal variation of nondimensional surface area for two different ambient conditions; comparison of predictions using the transient (TS) and quasisteady (QS) models with experimental data from Ref. [35]

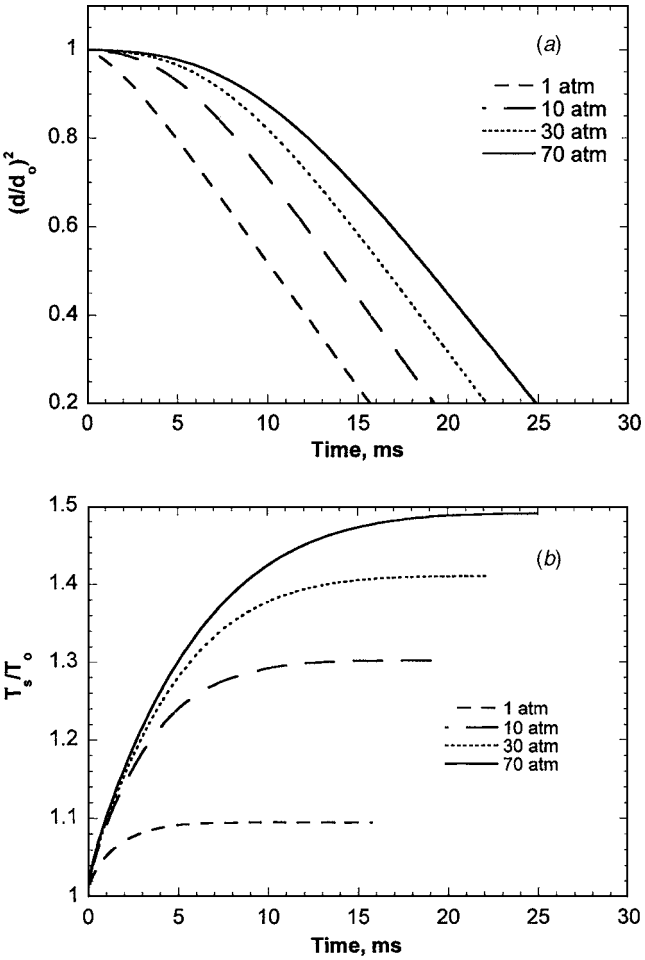

Fig. 4 Temporal histories of nondimensional surface area and temperature predicted using the QS models at different ambient pressures for T_a=500 K; (*a*) surface area and (*b*) surface temperature. The initial droplet diameter (d_0) is 0.05 mm and temperature (T_0) is 300 K.

transient (TS) models with the experimental data taken from Ref. [35]. The details of the TS model are to be found in our previous papers [26,36]. Results are presented in terms of the temporal variation of nondimensional surface area for two different ambient conditions. For the QS model, when pressure is low, i.e., 5 atm, the results agree reasonably well with the results of both the TS model and measurements. However, at high pressure, i.e., 50 atm, the predictions of both QS and TS models exhibit some differences from the measurements. The QS model underpredicts the surface regression rate during the early part of droplet lifetime and overpredicts it during the later part of the lifetime, as discussed in the next section. Apart from this difference, the predictions of both the QS and TS models as well as the measurements indicate that after the transient heating period, the surface regression rate nearly follows the d^2-law behavior. The results also show that as the pressure increases, the droplet heatup time becomes a more significant part of droplet lifetime, since the liquid boiling temperature increases with pressure.

Results of QS Model. In order to assess the applicability of the high-pressure QS model, several results are now presented using the QS model. The initial droplet temperature is 300 K. The ambient temperature and pressure range between 500–1500 K and l–70 atm, respectively. The initial droplet diameter is 0.05 mm. These ranges cover the environmental states of *n*-heptane fuel droplet and include the conditions in which practical droplets and sprays evaporate.

Figure 4(*a*) shows the temporal variation of nondimensional surface area obtained using the QS model for four different ambient pressures at 500 K. The droplet lifetime increases as the ambient pressure is increased. This can be directly attributed to the increase in droplet heat-up time with pressure, since the fuel boiling temperature increases with pressure. As indicated in Fig. 4(*b*), the heat-up time increases as ambient pressure is increased, and becomes a more significant part of droplet lifetime at high pressures. These results agree qualitatively with those of previous studies [17,26]. It is also interesting to note that following the transient heatup period, during which the droplet surface reaches the wet-bulb temperature, the surface regression nearly follows the d^2-law behavior, and the evaporation rate constant is nearly independent of pressure. At low ambient temperature, the transient effect is caused mainly by the liquid-phase heating. Consequently, as the pressure is increased, it increases the droplet heat-up time, and, thereby, the droplet lifetime.

Results concerning the effect of pressure on droplet vaporization at higher ambient temperature are presented in Figs. 5 and 6. The comparison of Fig. 4 with Figs. 5 and 6 indicates that the effect of pressure on vaporization is markedly different at low and high ambient temperatures. The global effect of pressure on droplet vaporization is presented in Fig. 7, which shows the variation of droplet lifetime with pressure at different ambient temperatures. As pressure is increased, the droplet lifetime increases at low T_a, but decreases at high T_a. At low T_a, the effect on pressure is predominantly due to its effect on the boiling temperature. Since the boiling temperature increases with pressure, the droplet heatup time increases, which in turn increases the droplet lifetime as indicated in Fig. 4. In contrast, at high T_a, the effect of pressure appears mainly through the heat of vaporization that decreases with pressure, and, consequently, the lifetime decreases. This is clearly indicated in Figs. 5 and 6.

Another important effect of pressure at higher ambient temperature pertains to the attainment of critical mixing state at the droplet surface. The critical mixing state, which is defined when the droplet surface temperature (T_s) attains the critical mixing temperature (T_{cm}) for a given ambient pressure, distinguishes between the subcritical and supercritical vaporization. For subcritical vaporization, $T_s < T_{cm}$, there is a distinct liquid-gas interface, and the vaporization is characterized by the regression of this interface. However, for $T_s \geq T_{cm}$, the distinction between the two phases disappears, and then the vaporization is generally characterized by the inward movement of the critical mixing surface. While the

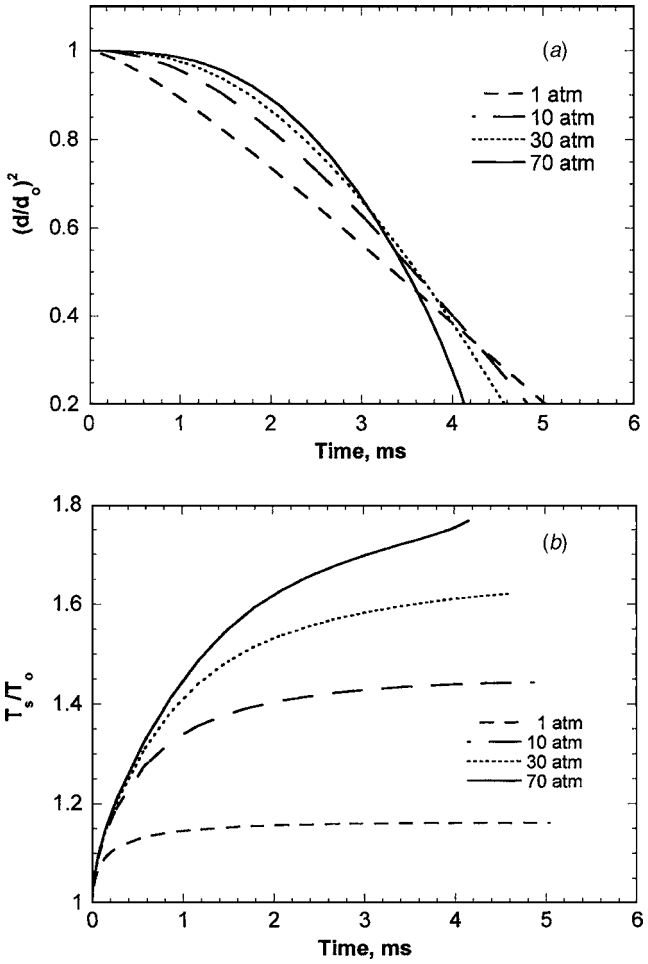

Fig. 5 Temporal histories of nondimensional surface area and temperature predicted using the QS models at different ambient pressures for T_a=1000 K; (*a*) surface area and (*b*) surface temperature

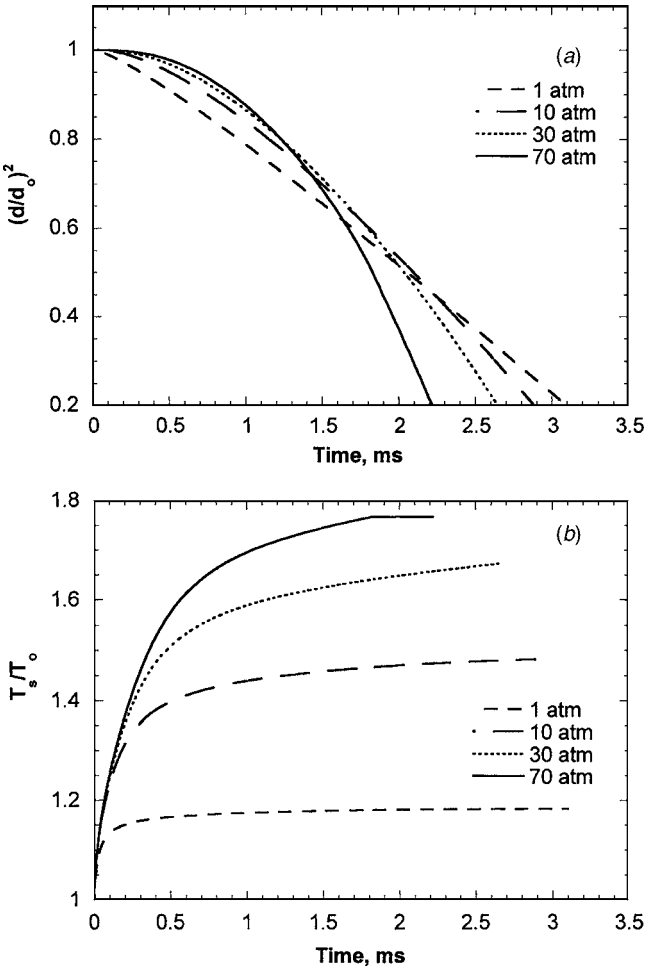

Fig. 6 Temporal histories of nondimensional surface area and temperature predicted using the QS models at different ambient pressures for T_a=1500 K; (*a*) surface area and (*b*) surface temperature

attainment of the critical mixing state has been discussed in the context of transient vaporization models [26,36], it has not been observed or discussed within the framework of quasisteady models. In Fig. 8 we present the final droplet surface temperature as a function of ambient pressure and temperature. In order to discuss the critical mixing state, the boiling line and the critical mixing line are also shown in the figure. At low T_a, as pressure is increased, the final surface temperature, which may be termed as the wet-bulb temperature, increases but does not reach the critical mixing value during the lifetime. However, at higher ambient temperature, the final surface temperature reaches the critical mixing state at some ambient pressure. The higher the ambient temperature, the lower is the value of pressure at which the droplet surface reaches the critical mixing state. The QS model is highly questionable for such conditions.

Comparison of Quasisteady (QS) and Transient (TS) Models. In Figs. 9 and 10, we compare the predictions of the QS and TS models for different ambient temperatures and pressures. The comparison is presented in terms of the temporal histories of nondimensional surface area and temperature obtained using the two models. In general, the differences between the predictions of the two models are relatively small at low to moderate pressures, but become noticeable at high pressures. The QS model underpredicts and overpredicts the droplet surface temperature and evaporation rate during the earlier and later part of droplet lifetime, respectively, compared to the TS model. The QS model also un-

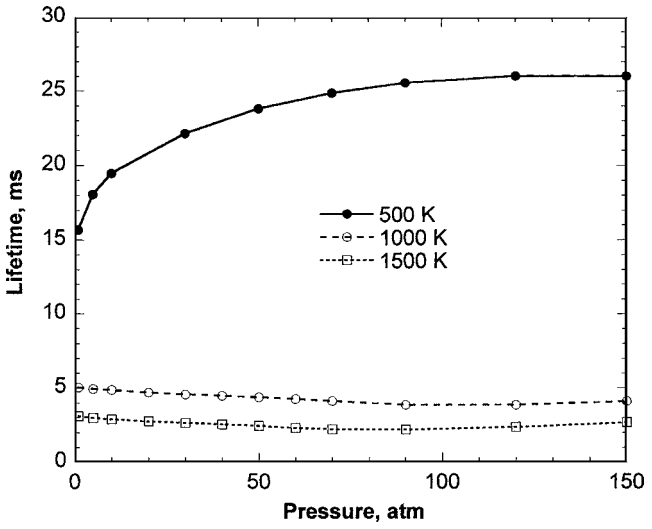

Fig. 7 Droplet lifetime versus pressure at different ambient temperatures

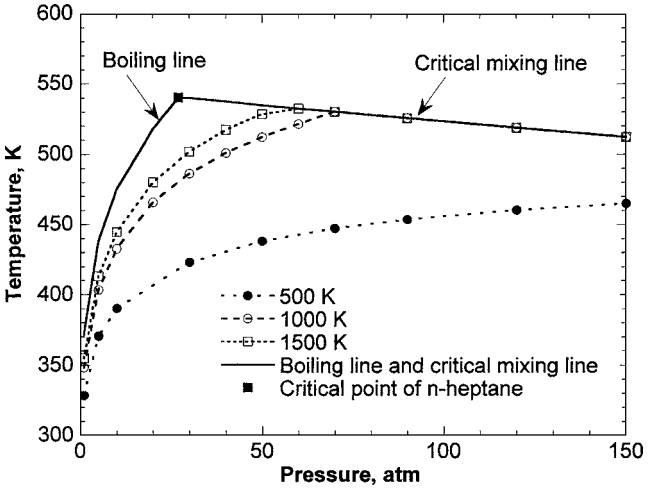

Fig. 8 Final droplet surface temperature plotted as a function of pressure for different ambient temperatures. The boiling line and critical mixing line are shown in the figure.

derpredicts the droplet lifetime compared to the TS model. As discussed in the following, these differences can be attributed to the quasisteady assumption in the QS model, since both the models employ the same algorithm for calculating the transport and

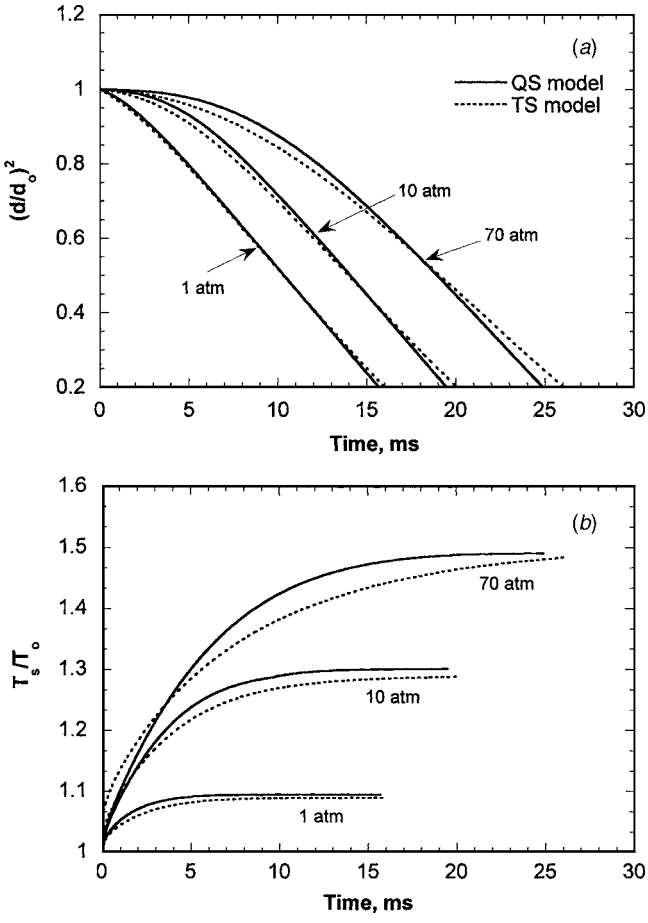

Fig. 9 Comparison of temporal histories of nondimensional surface area and temperature predicted using the QS and TS models at three different ambient pressures. (*a*) Surface area and (*b*) surface temperature. T_a=500 K. The initial droplet diameter (d_0) is 0.05 mm and temperature (T_0) is 300 K.

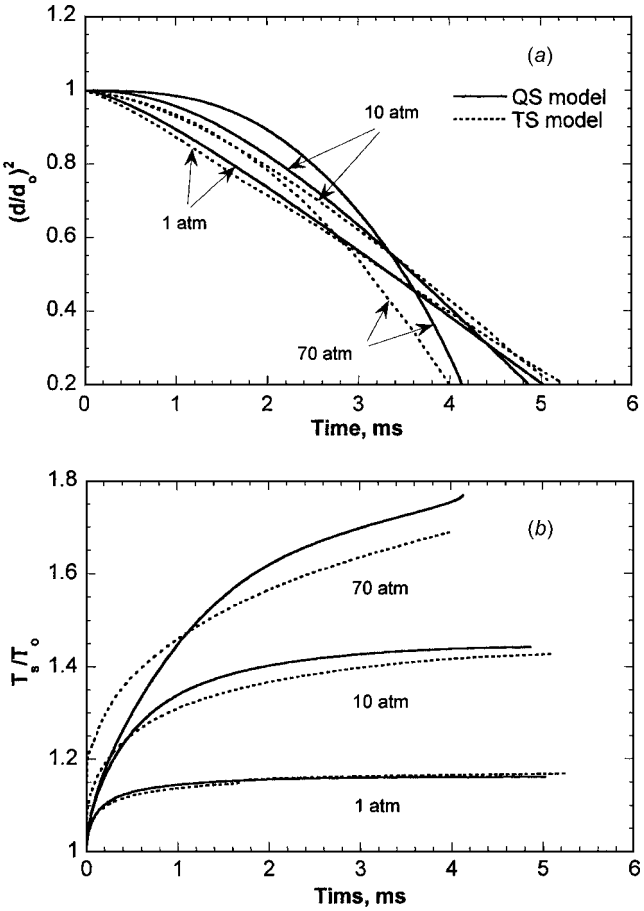

Fig. 10 Comparison of temporal histories of nondimensional surface area and temperature predicted using the QS and TS models at three different ambient pressures. (*a*) Surface area and (*b*) surface temperature. T_a=1000 K. The initial droplet diameter (d_0) is 0.05 mm and temperature (T_0) is 300 K.

thermodynamic properties.

Initially at $t=0$, as the droplet is introduced into the hot ambient, the gas film thickness, i.e., the gas layer between the droplet surface and gas ambient, is zero. Consequently, for the TS model, there is a large temperature gradient between high-temperature ambient gas and droplet surface, which results in high heat flux from the gas phase to the droplet surface. Since this effect is captured in the TS model, but not in the QS model that computes the heat flux using a suitable average of the droplet surface and ambient temperatures, it leads to higher droplet surface temperature for the TS model compared to the QS model, as indicated in Figs. 9(*b*) and 10(*b*). Consequently, the QS model underpredicts the evaporation rate during the early part of droplet lifetime compared to the TS model, as indicated in Figs. 9(*a*) and 10(*a*). Also note that for the QS model, the gas thermal conductivity is computed by using an average gas temperature and composition; see Eq. (16). The averaging procedure, which employs the one-third rule, implicitly assumes a gas-film thickness that is significantly larger than the actual value during the early part of drop lifetime. This leads to lower average gas temperature and higher fuel vapor mass fraction. While the lower gas temperature results in lower gas thermal conductivity and the higher fuel vapor mass fraction results in higher gas thermal conductivity, the net effect is the lower gas thermal conductivity, which leads to lower surface temperature for the QS model initially.

As the vaporization proceeds, the thickness of gas film for the TS model increases with time, which results in a smaller heat flux to the droplet surface. In contrast, for the QS model, the average

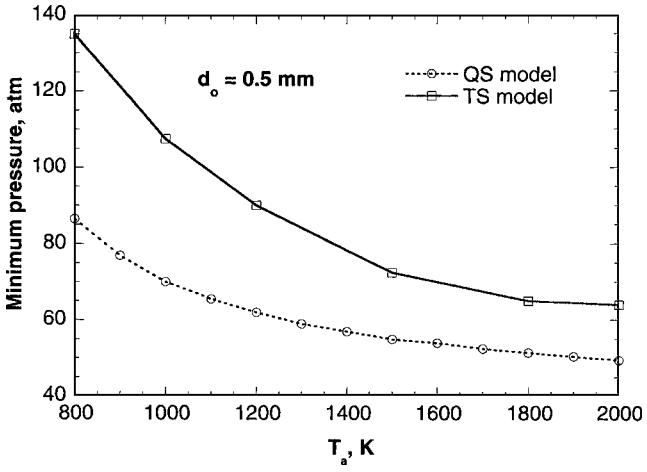

Fig. 11 Minimum pressure required for an *n*-heptane fuel droplet to attain the critical mixing state, plotted as a function of ambient temperature

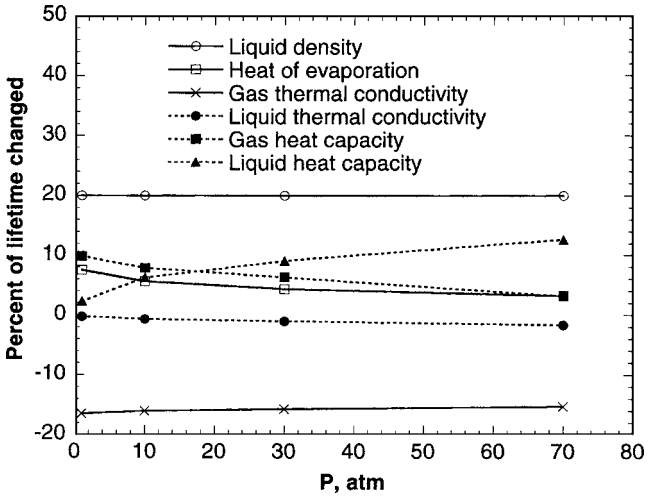

Fig. 12 Variation of droplet lifetime, resulting from an increase of a given property by 20%, plotted versus pressure for T_a = 1000 K

gas–film temperature increases as the droplet surface temperature increases with time. This leads to an overprediction of heat flux from the ambient gas to the droplet surface. As a consequence, during the later part of droplet lifetime, the surface temperature for the QS model is higher than that for the TS model. This also results in a higher fuel vapor mass fraction, and, consequently, higher gas thermal conductivity and higher evaporation rate during the later part of drop lifetime for the QS model. Additional results were obtained for both the QS and TS models by changing the initial droplet diameter. The differences between the predictions of the two models were found to be essentially independent of the initial droplet size.

An important aspect of high pressure vaporization is that the droplet surface may reach the critical mixing state during its lifetime, depending upon the ambient temperature and pressure. The transcritical vaporization behavior and the attainment of the critical mixing state in the context of transient model have been examined by several investigators [14–23]. Zhu and Aggarwal [26] quantified this behavior by plotting the minimum pressure required for the droplet surface to attain the critical mixing state as a function of ambient temperature. Figure 11 presents similar plots for both the QS and TS models. In order to obtain the minimum pressure value at a fixed ambient temperature, simulations were performed with increasingly higher pressures until the critical mixing state was observed at the droplet surface near the end of the droplet lifetime. As seen from the figure, the QS model predicts a vaporization process that reaches the critical mixing state at a significantly lower ambient pressure compared to that for the TS model. This is attributable to the fact that the QS model predicts higher surface temperature compared to the TS model during the later part of droplet lifetime.

The Effect of Thermotransport Properties on Vaporization Rate. Due to the importance of the gas- and liquid-phase properties to predict accurately the process of vaporization, we performed a sensitivity analysis to quantify as to which thermotransport property has the most influence on the predictions of the QS model. The sensitivity analysis is performed by increasing the value of a given property by 20%, and then examining its effect on droplet lifetime. Figure 12 shows the variations of droplet lifetime, resulting from an increase of a given property by 20%, plotted as a function of pressure at an ambient temperature of 1000 K. The droplet lifetime is most sensitive to liquid density and gas thermal conductivity. Increasing the liquid density by 20% increases the lifetime by 20%, since more energy is needed for liquid heating and vaporization. In contrast, increasing the gas thermal conductivity by 20% decreases the droplet lifetime by 16%, since higher gas thermal conductivity results in higher heat flux to the droplet, and thus a shorter lifetime. Other important properties are gas- and liquid-phase heat capacity and heat of vaporization. The droplet lifetime increases with increasing either of the heat capacities, since it lowers the liquid temperature. Increasing the heat of evaporation increases the lifetime, since more energy is needed for evaporation. In addition, the sensitivity of droplet lifetime to these three properties increases at higher pressures. The liquid thermal conductivity affects the droplet surface temperature through its influence on temperature distribution inside the droplet. However, the droplet lifetime is not affected noticeably by a 20% change in liquid thermal conductivity. Finally, it should be noted that the gas density and mass diffusivity change significantly with pressure.

High-Pressure Effects on Thermo-Transport Properties. An important issue in the context of developing a high-pressure vaporization model deals with the high-pressure effects on thermotransport properties. The high-pressure effects considered in the present study include gas-phase nonidealities, solubility of gases into liquid, high-pressure phase equilibrium at the droplet surface, transient liquid-phase heating, and high-pressure effects on thermotransport properties. The first four effects are clearly important, and have been modeled fairly accurately in the present study. Regarding the last effect, it is important to quantify as to which thermotransport property is most sensitive to the high-pressure effect. Our results indicate that the effect of pressure and temperature on the heat of vaporization should be represented accurately. The high-pressure effects on gas-phase thermal conductivity and specific heat become important for gas temperatures near the critical mixing point, but are negligible for higher temperatures.

The Effects of the Averaging Rule for Gas Temperature and Composition. The QS model generally uses the one-third rule to obtain the average gas temperature and composition, which are then used for calculating the thermotransport properties. As discussed in preceding sections, this leads to an underprediction of droplet surface temperature and, hence, of vaporization rate during the early part of drop lifetime, and their overprediction during the later part of lifetime for the QS model compared to that for the TS model. The underprediction and overprediction become more significant at higher ambient pressure and temperature. In order to reduce this error, a variable averaging factor should be used. During the early part of drop lifetime, a larger value should be used, while during the later part, a smaller value should be used. In

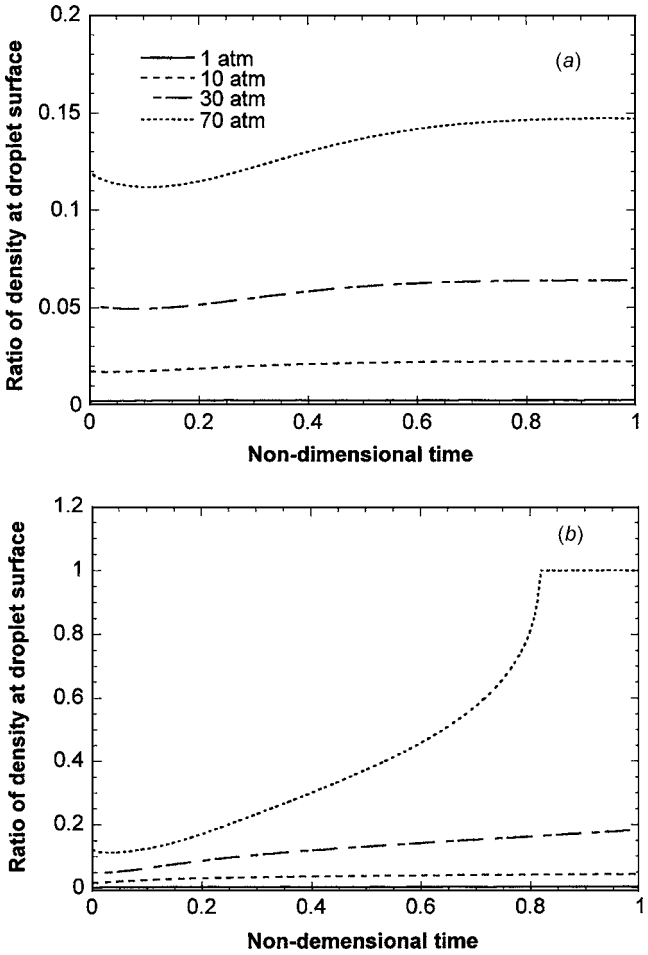

Fig. 13 Temporal variation of the ratio of gas density (at the droplet surface) to liquid density plotted versus pressure. (*a*) T_a=500 K, (*b*) T_a=1500 K.

addition, the higher the pressure and/or temperature, the larger the amount by which the averaging factor should be changed during the droplet lifetime.

The Range of Applicability of the QS Model. The justification for using the quasisteady model is based on the consideration that the gas density is much smaller than the liquid density [4]. In Fig. 13, the ratio of gas density to liquid density at the droplet surface is plotted versus the time, normalized by the corresponding lifetime, at different pressures. In accordance with the results presented earlier, the ratio is small at lower pressures, but becomes increasingly more significant at higher pressures. In addition, this ratio depends strongly on ambient temperature, and the effect becomes more significant at higher pressures.

In Fig. 14, we plot the final ratio (the final value corresponds to the time at which the droplet nondimensional surface area is 0.2) of gas density to liquid density as a function of pressure at three different ambient temperatures. At low ambient temperature, the final ratio linearly increases with pressure, but has a relatively small value even at very high pressures. In contrast, at high ambient temperature, the final ratio increases rapidly as the pressure exceeds the fuel critical pressure, and approaches unity as the critical mixing state is reached. This indicates that the quasisteady assumption becomes increasingly questionable as the ambient pressure exceeds the fuel critical pressure at high ambient temperature.

To obtain the range of applicability for the QS model, we plot in Fig. 15 the maximum pressure for which the final ratio of gas density to liquid density is smaller than 0.2 as a function of ambient temperature. The maximum pressure decreases as ambient temperature is increased, and approaches a constant value near the critical pressure. This indicates that the QS model can be used for a wide range of pressures at low ambient temperature, and for pressure up to the fuel critical pressure at high ambient temperature. The effect of droplet size is also shown in the figure, which indicates that the maximum pressure for the applicability of the QS model is independent of the initial droplet size.

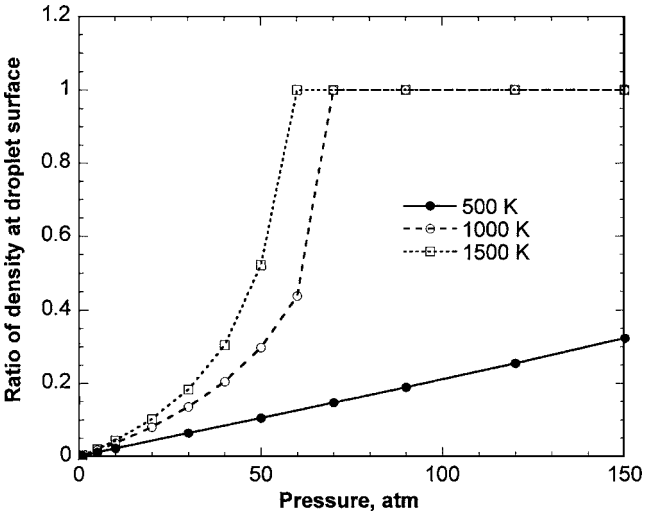

Fig. 14 The final ratio of gas density (at the droplet surface) to liquid density plotted versus pressure at different ambient temperatures

Conclusions

A quasisteady, high-pressure droplet gasification model has been developed and evaluated under conditions pertinent to high-pressure conditions in diesel and gas turbine combustors. The model includes a realistic representation of the high-pressure effects, and still is sufficiently simplified so that it can easily be incorporated into comprehensive spray codes. While the model retains the quasisteady gas-phase assumption, it considers the transient liquid-phase, transport inside the droplet. In addition, all the high-pressure effects are incorporated into the model. These include gas-phase nonidealities, solubility of gases into liquid, high-pressure phase equilibrium at the droplet surface, and depen-

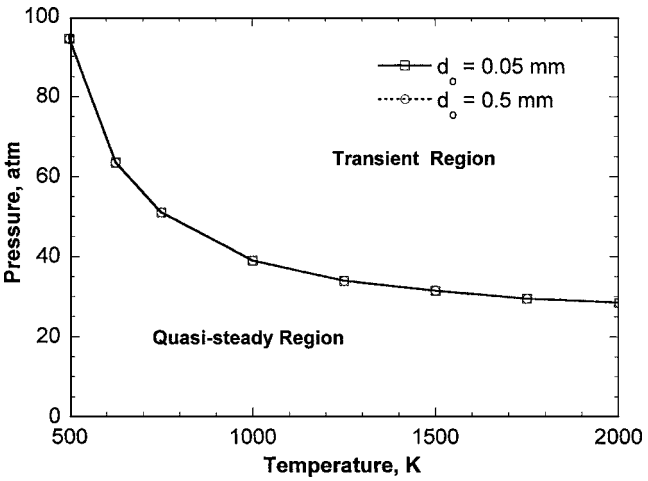

Fig. 15 The range of applicability of the QS model in terms of the limiting pressure plotted as a function of ambient temperature

dency of the gas- and liquid-phase properties on pressure. The validity of the quasisteady model is examined by comparing its predictions with those using a more comprehensive transient droplet model, as well as with the available experimental data. Based on these comparisons, the applicability of the quasisteady assumption is quantified in terms of ambient pressures and temperatures. Important conclusions are as follows:

1. There is a fairly good agreement between the QS and TS models for a wide range of pressures at low ambient temperatures, and for pressures up to the fuel critical pressure at high ambient temperature. Thus, the QS model developed in the present study can be used reliably for a relatively wide range of pressures at low ambient temperature, and for pressure up to the fuel critical pressure at high ambient temperature.
2. Compared to the TS model, the QS model predicts a lower evaporation rate initially and a higher rate during the later period of drop lifetime. This is mainly due to the assumption of gas-phase quasisteadiness and the averaging rule used in the QS model, which lead to smaller and larger gas-phase heat flux at the droplet surface, and thus lower and higher droplet surface temperature during the early and later periods of lifetime, respectively. The differences between the predicted evaporation rates using the two models become more significant at higher ambient temperatures and pressures. In addition, the vaporization process predicted using the QS model reaches the critical mixing state earlier, i.e., at lower ambient temperature and/or pressure than that predicted with the TS model. This is due to the higher droplet surface temperature predicted during the later part of drop lifetime for the QS model.
3. The droplet lifetime is very sensitive to the gas thermal conductivity and liquid density. Increasing the gas thermal conductivity or decreasing the liquid density decreases the lifetime. Other important properties are gas- and liquid-phase heat capacity. The lifetime increases with increasing either heat capacity.
4. Since the gas–film thickness changes during droplet lifetime, the QS model can be further refined by using a variable averaging factor for calculating the average gas temperature and composition used to compute the gas-phase thermotransport properties. During the early part of droplet lifetime, a larger value should be used, while during the later part, a smaller value should be used. In addition, the higher the ambient pressure and/or temperature, the larger the amount by which the averaging factor should be changed during droplet lifetime [37].

Acknowledgment

This research was partially funded by the GE Aircraft Engines. The code for the unsteady droplet model was provided by G. S. Zhu of Detroit Diesel Corporation. Many fruitful discussions with G. S. Zhu are also appreciated.

Nomenclature

a,b,A^*,B^* = dimensionless parameters for Peng–Robinson equation of state
B = transfer number
C_p = specific heat at constant pressure (kJ/kg K)
d = droplet diameter (mm)
D = mass diffusivity (m^2/s)
H = energy supplied to the droplet per unit mass of fuel vaporized (kJ/kg)
$\bar{H}$ = enthalpy of vaporization (kJ/kmol)
k = thermal conductivity (W/m K)
k_{ij} = binary interaction coefficient for Peng–Robinson equation of state
L = latent heat of vaporization (kJ/kg)
Le = Lewis number
$\dot{m}$ = evaporation rate (kg/s)
$\bar{m}$ = normalized evaporation rate
n = mole number
P = pressure (atm)
r = radial coordinate
$\bar{r}$ = normalized radial coordinate
R = gas constant (kJ/kg K)
t = time (s)
$\bar{t}$ = normalized temporal variable
T = temperature (K)
$\bar{T}$ = normalized temperature
V = molar volume (m^3/mol)
x = liquid mole fraction
y = vapor mole fraction
Y = vapor mass fraction
Z = compressibility factor

Greek Symbols

ρ = density (kg/m^3)
α = thermal diffusivity (m^2/s)
ϕ = fugacity coefficient
Φ = averaging gas temperature or mass fraction
β = averaging factor

Superscript

0 = ideal state
v = vapor
l = liquid

Subscript

a = ambient
avg = average
b = boiling point
c = critical point
f = fuel
g = gas
i, j = species i or j
l = liquid
s = droplet surface
o = initiate state
∞ = infinity or ambient

References

[1] Godsave, G. A. E., 1953, "Studies of the Combustion of Drops in a Fuel Spray—The Burning of Single Drops of Fuel," Fourth Symposium (International) on Combustion, Williams and Wilkins, Baltimore, pp. 818–830.
[2] Spalding, D. B., 1953, "The Combustion of Liquid Fuels," Fourth Symposium (International) on Combustion, Williams and Wilkins, Baltimore, pp. 847–864.
[3] Williams, A., 1973, "Combustion of Droplet of Liquid Fuels: A Review," Combust. Flame, **21**, pp. 1–31.
[4] Law, C. K., 1982, "Recent Advances in Droplet Vaporization and Combustion," Prog. Energy Combust. Sci., **8**, pp. 171–201.
[5] Sirignano, W. A., 1983, "Fuel Droplet Vaporization and Spray Combustion," Prog. Energy Combust. Sci., **9**, pp. 291–322.
[6] Peng, F. and Aggarwal, S. K., 1995, "A Review of Droplet Dynamics and Vaporization Modeling for Engineering Calculations," ASME J. Eng. Gas Turbines Power, **117**, pp. 453–461.
[7] Sirignano, W. A., 1979, "Theory of Multicomponent Fuel Droplet Vaporization," Archives of Thermodynamics and Combustion, **9**, pp. 231–251.
[8] Aggarwal, S. K., Tong, A., and Sirignano, W. A., 1984, "A Comparison of Vaporization Models in Spray Calculations," AIAA J., **22**, pp. 1448–1457.
[9] Abramzon, B. and Sirignano, W. A., 1989, "Droplet Vaporization Model for Spray Combustion Calculations," Int. J. Heat Mass Transfer, **32**, pp. 1605–1618.
[10] Faeth, G. M., 1983, "Evaporation and Combustion of Sprays," Prog. Energy Combust. Sci., **9**, pp. 1–76.
[11] Aggarwal, S. K., 1987, "Modeling of Multicomponent Fuel Spray Vaporization," Int. J. Heat Mass Transfer, **30**, pp. 1949–1961.
[12] Aggarwal, S. K., Shu, Z., Mongia H. and Hura, H. S., 1998, "Multicomponent Fuel Effects on the Vaporization of a Surrogate Single-Component Fuel Droplet," ASME Paper No. 98-0157.
[13] Matlosz, R. L., Leipziger, S., and Torda, T. P., 1972, "Investigation of Liquid

Drop Evaporation in a High Temperature and High Pressure Environment," Int. J. Heat Mass Transfer, **15**, pp. 831–852.
[14] Hsieh, K. C., Shuen, J. S., and Yang, V., 1991, "Droplet Vaporization in High-Pressure Environment, I: Near-Critical Conditions," Combust. Sci. Technol., **76**, pp. 111–132.
[15] Curtis, E. W. and Farrell, P. V., 1992, "A Numerical Study of High-Pressure Droplet Vaporization," Combust. Flame, **90**, pp. 85–102.
[16] Shuen, J. S., Yang, V., and Hsiao, C. C., 1992, "Combustion of Liquid-Fuel Droplets in Supercritical Conditions," Combust. Flame, **89**, pp. 299–319.
[17] Jia, H. and Gogos, G., 1993, "High Pressure Droplet Vaporization; Effects of Liquid-Phase Gas Solubility," Int. J. Heat Mass Transfer, **36**, pp. 4419–4431.
[18] Yang, V., Lin, N. N., and Shuen, J. S., 1994, "Vaporization of Liquid Oxygen (LOX) Droplets in Supercritical Hydrogen Environments," Combust. Sci. Technol., **97**, pp. 247–270.
[19] Givler, S. D. and Abraham, J., 1996, "Supercritical Droplet Vaporization and Combustion Studies," Prog. Energy Combust. Sci., **22**, pp. 1–28.
[20] Curtis, E. W., Ulodogan, A. and Reitz, R. D., 1995, "A New High Pressure Droplet Vaporization Model for Diesel Engine Modeling," SAE Paper No. 952431.
[21] Abraham, J. and Givler, S. D., 1999, "Conditions in Which Fuel Drops Reach a Critical State in a Diesel Engine," SAE Paper No. 1999-01-0511.
[22] Sirignano, W. A. and Delplanque, J.-P., 1999, "Transcritical Vaporization of Liquid Fuels and Propellants," AIAA J., **15**, pp. 896–902.
[23] Yang, V., 2000, "Modeling of Supercritical Vaporization, Mixing, and Combustion Processes in Liquid-Fueled Propulsion System," Proc. of the Combustion Institute, Vol. 28, pp. 925–942.
[24] Sirignano, W. A., 1999, *Fluid Dynamics and Transport of Droplets and Sprays*, Cambridge University Press, Cambridge, UK.
[25] Aggarwal, S. K., and Mongia, H., 2002, "Multicomponent and High-Pressure Effects on Droplet Vaporization," ASME J. Eng. Gas Turbines Power, **124**, pp. 248–257.
[26] Zhu, G. and Aggarwal, S. K., 2000, "Transient Supercritical Droplet Evaporation with Emphasis on the Effects of Equation of State," Int. J. Heat Mass Transfer **43**, pp. 1157–1171.
[27] Reid, R. C., Prausnitz, J. M., and Poling, B. E., 1987, *The Properties of Gases and Liquids*, McGraw-Hill, New York.
[28] Knapp, H., Doring, R., Oellrich, L., Plocker, U. and Prausnitz, J. M., 1982, *Vapor-Liquid Equilibria for Mixture of Low Boiling Substances, Chemical Engineering Data Series*, Vol. VI, Dechema, Frankfurt.
[29] Filippov, L. P., 1955,"Thermal Conduction of Solutions in Associated Liquids: Thermal Conduction of 50 Organic Liquids," Chem. Abstr. **49**, Col. 15430–15431; Chem. Abstr. 1956, **50**, Col. 8276.
[30] Baroncini, C., Di Filippo, P., and Latini, G., 1983, "Comparison Between Predicted and Experimental Thermal Conductivity Values for the Liquid Substances and the Liquid Mixtures at Different Temperatures and Pressures," paper presented at the Workshop on Thermal Conductivity Measurement, IMEKO, Budapest.
[31] Chung, T. H., Ajlan, M., Lee, L. L., and Starling, K. E., 1988, "Generalized Multiparameter Correlation for Nonpolar and Polar Fluid Transport Properties," Ind. Eng. Chem. Res. **27**, pp. 671–679.
[32] Chung, T. H., Lee, L. L., and Starling, K. E., 1984, "Applications of Kinetic Gas Theories and Multiparameter Correlation for Prediction of Dilute Gas Viscosity and Thermal Conductivity," Ind. Eng. Chem. Fundam., **23**, pp. 8–13.
[33] Takahashi, S., 1974, "Preparation of a Generalized Chart for the Diffusion Coefficients of Gases at High Pressures," J. Chem. Eng. Jpn., **6**, pp. 417–420.
[34] Vargaftik, N. B., 1983, *Handbook of Physical Properties of Liquids and Gases, Pure Substances and Mixtures*, 2nd ed., Hemisphere, New York.
[35] Nomura, H., Ujiie, Y., Rath, H. J., Sato, J., and Kono, M., 1996, "Experimental Study of High-Pressure Droplet Evaporation Using Microgravity Conditions," Twenty-Sixth Symposium (International) on Combustion, The Combustion Institute, pp. 1267–1273.
[36] Zhu, G. S., Reitz, R. D., and Aggarwal, S. K., 2001, "Gas-phase Unsteadiness and Its Influence on Droplet Vaporization in Sub- and Super-critical Environments," Int. J. Heat Mass Transfer, **44**, pp. 3081–3093.
[37] Zhu, G.-S., and Reitz, R. D., 2001, "Engine Fuel Droplet High-Pressure Vaporization Modeling," ASME J. Eng. Gas Turbines Power, **123**(2), pp. 412–418.